RSC Advances

PAPER

View Article Online
View Journal | View Issue

Open Access Article. Published on 23 July 2025. Downloaded on 11/8/2025 4:52:06 AM.
This article is licensed under a Creative Commons Attribution-NonCommercial 3.0 Unported Licence.

Check for updates

Cite this: *RSC Adv.*, 2025, **15**, 26362

Hydrogel particle-based protein display enabled by particle-templated emulsification†

Han Wu, * Jiayao Fang, Jiao Chen, Yaoqi Wang and Bo Zheng *

Protein display technology enables high-throughput screening and plays an important role in protein discovery and engineering. Conventional *in vivo* display methods face challenges such as inefficient gene transformation and complex cell proliferation dynamics, while *in vitro* display methods are often limited to affinity-based selection and suffer from expression bias due to homogeneous reaction conditions. Here, we present a hydrogel particle-based protein display method enabled by particle-templated emulsification. This approach uses functionalized polyacrylamide hydrogel particles as isolated microreactors, incorporating DNA primers for genotype immobilization and Ni-NTA groups for capturing histidine-tagged protein phenotypes. Displayed proteins are synthesized *via* cell-free protein expression within isolated droplets, overcoming the limitations of *in vivo* cell culture and enabling compartmentalized screening, which is challenging in conventional homogeneous *in vitro* systems. Using particle-templated emulsification, single hydrogel particles can be rapidly encapsulated with individual DNA templates into isolated water-in-oil droplets within 30 seconds, without the need for specialized instrumentation. Up to 10^9 particles can be emulsified in a standard 50 ml conical tube. Compared to conventional droplet microfluidics, particle-templated emulsification achieves higher single-particle encapsulation and improved one-to-one particle–DNA pairing efficiency, reducing reagent consumption and minimizing DNA library loss caused by improper pairing. Digital PCR and cell-free protein expression are sequentially performed within droplets, with both the amplified DNA and the expressed protein immobilized on the same particle, thereby establishing a stable genotype–phenotype linkage. This method eliminates the need for cell handling, enables compartmentalized functional screening, and provides a fast, scalable, and user-friendly workflow for protein display, offering strong potential in directed evolution and protein engineering.

Received 23rd May 2025
Accepted 16th July 2025

DOI: 10.1039/d5ra03622d

rsc.li/rsc-advances

1. Introduction

Proteins are essential biomolecules with broad and significant applications in health research,[1,2] drug discovery,[3,4] industry catalysis,[5,6] and biotechnology development.[7,8] Their diverse functions and vital roles in biological systems have driven researchers to design and engineer proteins with novel properties not found in nature, tailored to suit the needs of industrial and biological applications.[9–12] The three primary approaches to protein engineering are *de novo* design, rational design and directed evolution.[12–14] These methods generally start from creating a library of genes with varied sequences encoding the target protein, followed by protein expression and screening. Subsequently, proteins with desired properties are selected and finally identified by retrieving the gene information.

Since proteins are usually expressed and reside within cells, screening and analyzing proteins can be challenging, as many screening reagents cannot freely cross the cell membrane. Lysing the host cells can facilitate protein screening and analysis, but raises problems of disrupting the physical linkages between proteins and their encoding genes. Therefore, it is necessary to develop techniques that expose expressed proteins to external environments for screening and analysis, while maintaining their physical linkages to the encoding genes.

To this purpose, various "display" methods have been developed to present expressed proteins on a surface and meanwhile couple genes with proteins.[15–17] Phage display and cell surface display are two powerful techniques for rapid protein discovery that effectively preserve the genotype–phenotype relationship by genetically modifying bacteriophages or cells to fuse target proteins to anchoring motifs on surfaces, such as phage coat proteins in phage display and carrier proteins in cell surface display.[18–22] However, in both methods, the target proteins are fused with the host's proteins, which can be constrained by the growth and viability of the host cells. Additionally, the limited transformation efficiency when

Institute of Chemical Biology, Shenzhen Bay Laboratory, Shenzhen, China. E-mail: wuhan@szbl.ac.cn; bozheng@szbl.ac.cn

† Electronic supplementary information (ESI) available. See DOI: https://doi.org/10.1039/d5ra03622d

© 2025 The Author(s). Published by the Royal Society of Chemistry

Open Access Article. Published on 23 July 2025. Downloaded on 11/8/2025 4:52:06 AM.
This article is licensed under a Creative Commons Attribution-NonCommercial 3.0 Unported Licence.

introducing genes into cells or phages can lead to a loss of genetic diversity.

In vitro display methods, such as mRNA display and ribosome display address the challenges of gene transformation and cell culture.[16,23–27] In mRNA display, the protein is covalently bonded to its encoding mRNA *via* a puromycin linkage after transcription and translation.[16,23] Ribosome display creates a protein–ribosome–mRNA ternary complex by eliminating the stop codon of mRNA, resulting in keeping the *in vitro* expressed protein on the ribosome instead of releasing it.[25–27] In both methods, mRNA serves as the gene information carrier and is involved in the entire screening and gene identification process. Consequently, the stability of mRNA is important, as it must keep intact for an extended period in a complex environment. Additionally, since both mRNA display and ribosome display are performed in a homogeneous phase, they are more suited for applications such as binding affinity selection, including antibody or ligand screening, but are not directly applicable to enzyme evolution, which requires compartmentalized gene–protein complexes to enable catalytic screening. Homogeneous reactions also carry an increased risk of biased protein expression due to competition for transcription and translation factors, which can potentially reduce the genetic diversity of the DNA library.[28,29]

To address these challenges, Lee *et al.* developed a method for displaying proteins on microbeads.[30] In the study, DNA encoding the target protein was pre-immobilized on microbeads, and the expressed protein by the DNA was subsequently captured and displayed on the same microbead by reacting with functional groups on its surface. This approach allowed protein expression to occur on individual microbeads, thus eliminating competition among different gene variants in homogeneous reactions. Byun *et al.* assembled a DNA array with a hydrogel matrix functionalized with protein capture sites.[31] After *in vitro* expression, a protein array was generated, displaying proteins on the hydrogel surface based on the DNA array as a template. However, both platforms faced challenges with high-throughput protein screening. In both studies, only a single genotype prepared by PCR was used, either immobilized on microbeads or spotted in the array. In Lee's work, ensuring that each of the numerous microbeads was immobilized with a single PCR-amplified genotype was challenging and difficult to scale. In Byun's work, although the method allowed for spatially resolved immobilization of different DNA genotypes on an array, the need to generate a large and diverse library of PCR products posed a significant limitation. Each genotype had to be individually amplified, purified, and deposited, resulting in a considerable bottleneck in terms of time, labour, and scalability. Therefore, display techniques that start with a single DNA template per genotype and enable efficient protein expression would be more effective and powerful.

Weitz and colleagues developed a hydrogel display method that combined digital PCR and cell-free protein expression.[32] In this method, hydrogel particles were first modified with PCR primers and protein anchor groups. These particles were then partitioned into water-in-oil droplets using microfluidics, with each droplet containing 1 or 0 DNA templates. After PCR, droplets containing both a hydrogel particle and a single DNA template generated hundreds of DNA copies immobilized on the hydrogel, as the primers for PCR were pre-immobilized. The droplets were then demulsified to remove PCR reagents and re-emulsified with cell-free protein expression reagents to form water-in-oil droplets again *via* microfluidics. After protein expression, the droplets were demulsified once more, resulting in the expressed protein and its encoding gene immobilized on the same hydrogel particle. This dual emulsification process enabled digital PCR and cell-free protein expression to occur separately and sequentially within individual microdroplets, providing optimal conditions for both reactions, thereby effectively eliminating expression bias and preserving gene diversity.

However, the dual emulsification process using microfluidics requires specialized microfluidics hardware and expertise, and it is time-intensive to generate a large number of droplets. Achieving encapsulation of a single hydrogel particle paired with one DNA template per droplet for digital PCR, or one particle per droplet for cell-free protein expression, often results in many improperly loaded droplets due to Poisson distribution.[33–36] Consequently, some DNA variants may be lost, as it is nearly impossible to ensure that each DNA variant in the library is paired with a single hydrogel particle within a droplet. Additionally, the inefficiency of single-particle and single-template pairing for digital PCR and single particle encapsulation for protein expression necessitates generating much larger numbers of droplets than the DNA library size itself, further increasing time demands for droplets generation. Here, we employed particle-templated emulsification to rapidly generate large numbers of monodispersed emulsions without microfluidics.[37–39] In the approach, hydrogel particles incubated with the sample solution were dispersed in an oil phase, followed by vigorous agitation to form emulsions. During agitation, aqueous droplets continuously broke into smaller ones until reaching the size of a single hydrogel particle, as further droplet breakup would require fracturing the solid hydrogel particles. This ensured that each droplet contained one hydrogel particle, with the droplet size closely matching the particle diameter. This particle-templated emulsification method allows for the generation of large numbers of droplets containing single hydrogel particles in about 30 seconds, while microfluidic droplet generation at a typical rate of 1 kHz would take over 11 hours to produce 2 ml of 40 μm-diameter droplets.[38] Additionally, the issue of sample loss during encapsulation was mitigated, as all samples were absorbed by the hydrogel particles and efficiently partitioned into emulsions.

Therefore, conventional *in vivo* display methods, such as cell surface display and phage display, face challenges including inefficient gene transformation and complex cell proliferation dynamics. *In vitro* display methods, such as ribosome display and mRNA display, are limited to binding affinity selection and are susceptible to protein expression bias due to the homogeneous reaction environment. Microfluidics-based hydrogel display methods address these limitations by generating isolated microreactors and integrating PCR and cell-free protein expression. However, current hydrogel display techniques often require multiple rounds of time-consuming droplet generation

Open Access Article. Published on 23 July 2025. Downloaded on 11/8/2025 4:52:06 AM.
This article is licensed under a Creative Commons Attribution-NonCommercial 3.0 Unported Licence.

for digital PCR and protein expression. Moreover, the pairing efficiency between single particles and single templates for digital PCR, as well as the encapsulation efficiency of single particles for protein expression are limited, leading to the loss of some DNA variants. To overcome these challenges, we developed a hydrogel-particle based protein display method enabled by particle-templated emulsification. Both DNA template amplification and protein expression are performed within isolated hydrogel particles, making the system well-suited for applications such as enzyme evolution, which requires compartmentalized screening. The particle-templated emulsification process, driven by simple, instrument-free agitation, rapidly encapsulates single particles into droplets in just 30 seconds, offering a significantly faster alternative to conventional droplet microfluidics. More importantly, the particle-templated emulsification would allow higher one-to-one pairing efficiency during encapsulation, thereby reducing the risk of DNA library loss.

2. Materials and methods

2.1 Chemicals and materials

Acrylamide/bis-acrylamide (30% solution, 19 : 1, BioReagent), ammonium persulfate (APS, ≥98% purity), Triton X-100 (Molecular Biology Grade), nickel(II) sulfate (≥98% purity), fluorescein isothiocyanate (FITC, ≥90% purity), sodium cyanoborohydride ($NaCNBH_3$, ≥95% purity), and *N*α,*N*α-bis(carboxymethyl)-L-lysine hydrate (AB-NTA, ≥97% purity) were purchased from Sigma-Aldrich. Glutaraldehyde (25% in H_2O) was obtained from Macklin. Hexamethylenediamine (≥99% purity) and *N*,*N*,*N*′,*N*′-tetramethylethylenediamine (TEMED, ≥99% purity) were obtained from Aladdin. HFE-7500 with 2% 008-FluoroSurfactant and FC-40 with 5% 008-FluoroSurfactant were purchased from RAN Biotechnologies. Drop-Surf droplet generation oil and droplet demulsifying agent were obtained from Suzhou Cchip Scientific Instrument Co., Ltd. Siloxane Sylgard 184 silicone elastomer kit was purchased from Dow Corning. Acrylate–PEG–NH_2 (average M_w 2000, ≥97% purity) was purchased from Beijing Mreda Technology Co., Ltd and phosphate buffered saline (PBS, pH 7.4, DNase, RNase & Protease free, Sterile) was obtained from Shanghai Kingmorn Biotechnology Co., Ltd.

The droplet digital PCR Multiplex Supermix was obtained from Bio-Rad. The *E. coli* S30 Extract System for Linear Templates kit was obtained from Promega Corporation. RNase inhibitor (murine) was purchased from New England Biolabs and EvaGreen dye was acquired from Yeasen Biotechnology. Creatine kinase was obtained from Roche. T7 polymerase and enhanced green fluorescent protein (EGFP) was expressed and purified by ourselves. Streptavidin conjugated horseradish peroxidase (HRP) and SignalUp Ultrasensitive ELISA Assay Kit with Fluorescence HRP Substrate were obtained from Beyotime. All primers for digital PCR and the pUC57-HoxAl plasmid were provided by GenScript, while the pIVEX2.4C-mCherry plasmid and pIVEX2.4C-EGFP plasmid were obtained from Miaoling Biology.

2.2 Hydrogel particles preparation

Hydrogel particles were prepared using a flow-focusing microfluidic chip[40–42] fabricated by photolithography and PDMS soft-lithography.[43,44] The aqueous phase consisted of 6.5% (w/v) acrylamide/bis-acrylamide, 0.45% (w/v) APS and 20 mg per ml acrylate–PEG–NH_2, and was injected into the microfluidic chip with the droplet generation oil containing 1% (v/v) TEMED serving as the continuous phase. The hydrogel precursor droplets were collected and incubated overnight at room temperature for gelation. The gelled droplets were then demulsified with a demulsifying agent and washed with PBS buffer containing 0.5% Triton X-100 to remove unreacted reagents.

2.3 Hydrogel particles functionalization

Hydrogel particles were incubated with 2.5% (v/v) glutaraldehyde for 2 hours at room temperature under continuous shaking, followed by thorough washing to introduce aldehyde groups onto the hydrogel surface for bioconjugation. Then, 0.8 μM 5′-amine-C12 modified forward and reverse primers were reacted with the aldehyde-functionalized hydrogels for covalent immobilization. Excess aldehyde groups were subsequently saturated with hexamethylenediamine after reacting for 2 hours at room temperature. Finally, the resulting Schiff bases formed between aldehyde and amine groups were stabilized with $NaCNBH_3$.

2.4 Particle-templated emulsification and digital PCR in hydrogel particles

Hydrogel particles were incubated with digital PCR mixtures containing 1× droplet digital multiplex supermix and 0.8 μM forward primer for 15 min to allow PCR reagents to diffuse into the particles. After centrifugation at 6000*g* for 1 min, excess PCR reagents in the aqueous phase were removed, and the DNA template solution was then added and mixed. Subsequently, HFE-7500 oil with 2% (w/w) 008-FluoroSurfactant was introduced and the mixture was pipetted and agitated by flicking to form hydrogel particle-in-oil droplets.[37–39] Finally, the oil phase was replaced with FC-40 oil with 5% 008-FluoroSurfactant to enhanced the droplets thermostability during PCR.

Digital PCR was performed in a C1000 Touch thermocycler (Bio-Rad) with the following program: 95 °C for 10 min, followed by 40 cycles of 94 °C for 30 s, and 60 °C for 1 min, with a final enzyme deactivation of 10 min at 98 °C, followed by holding at 4 °C. Droplets were then demulsified and washed to remove PCR reagents. To observe the digital PCR results, the particles were incubated with 1× EvaGreen, washed and then observed under a fluorescent microscope.

2.5 Cell-free protein expression in hydrogel particles

After digital PCR, hydrogel particles were modified with glutaraldehyde again by incubating with 2.5% (v/v) glutaraldehyde for 2 hours at room temperature through reacting with the amine groups of hexamethylenediamine. After washing, the

 © 2025 The Author(s). Published by the Royal Society of Chemistry

Open Access Article. Published on 23 July 2025. Downloaded on 11/8/2025 4:52:06 AM.
This article is licensed under a Creative Commons Attribution-NonCommercial 3.0 Unported Licence.

hydrogel particles were sequentially functionalized with AB-NTA and $NiSO_4$ to immobilize Ni-NTA groups on the hydrogel.

The hydrogel particles were then dehydrated by lyophilization and rehydrated in a cell-free protein expression mixture, which was prepared according to the manufacturer's protocol.[45–47] For a 20 μl mixture, the composition included 2 μl amino acid mixture, 8 μl S30 premix without amino acids, 6 μl S30 extracts, 1 μl T7 polymerase, 1 μl creatine kinase, 1 μl RNase inhibitor, and 1 μl water. After rehydration, excess cell-free protein expression mixture was removed, and particle-templated emulsification was performed following the same procedure as digital PCR, with the exception that HFE-7500 oil with 2% (w/w) 008-FluoroSurfactant was not replaced with FC-40 oil with 5% 008-FluoroSurfactant, since the reaction temperature for cell-free protein expression was not high. The emulsions were then incubated at 30 °C for 6 hours to allow protein expression. Finally, the emulsions were demulsified and washed to remove any unconjugated molecules from the hydrogel particles. To observe the cell-free protein expression results, hydrogel particles in PBS buffer were added on a glass slide and examined under a fluorescent microscope.

3. Results and discussion

3.1 Working principle of the hydrogel display

As shown in Fig. 1, we first functionalized hydrogel particles with primers and encapsulated each particle with a single DNA template in droplets using particle-templated emulsification. After PCR, the droplets were demulsified and the hydrogel particles were further modified with Ni-NTA groups, which exhibit strong binding affinity for histidine-tagged proteins. The particles were then incubated with cell-free protein expression reagents and re-emulsified *via* particle-templated emulsification. The expressed histidine-tagged proteins were subsequently immobilized on the particles through binding to the Ni-NTA groups, thereby achieving protein display on the hydrogel particles.

In protein display, proteins with various phenotypes are expressed from a DNA template library, which is typically large to encode more proteins for selection. However, each DNA variant may yield different amounts of protein products, leading to potential selection bias. For instance, in mRNA display and ribosome display, proteins are expressed in a homogeneous phase, competing for transcription and translation factors, which can result in expression bias.[28,29] In this study, we implemented several methods to eliminate the expression bias. First, reactions were conducted within separated individual particles with ample reagents, thus avoiding competition for reaction reagents. Single DNA templates were emulsified with a single hydrogel particle for digital PCR, followed by transcription and translation into target proteins within each isolated particle. This isolated environment with sufficient reaction reagents allowed each reaction to reach its full potential. Second, pre-amplification of the DNA library was important, as cell-free protein expression from a single DNA template can be unstable and produce inconsistent yields.[48] Digital PCR which amplifies single DNA templates is more robust, providing hundreds of DNA copies for each genotype, which helps to eliminate bias in cell-free protein expression.

Another important issue in protein display is maintaining the linkage between genotype and phenotype, *i.e.*, the expressed protein and its encoding gene throughout the assay. Here, hydrogel particles were first functionalized with primers for DNA amplification and amine groups which are stable during PCR while allowing for further functionalization (Fig. 1). After particle-templated emulsification, single DNA templates in droplets were amplified to produce hundreds of DNA copies attached to the hydrogel. The droplets were then demulsified and Ni-NTA groups were introduced onto the hydrogel through multi-step functionalization with amine groups. Following incubation with cell-free protein expression reagents, the hydrogel particles were re-emulsified and the expressed proteins were captured by the Ni-NTA groups, and displayed on the hydrogel. As a result, the expressed protein and its encoding gene were both immobilized on the same hydrogel particle, with no cross-contamination between hydrogel particles, as both PCR and cell-free protein expression occurred within droplets containing a single hydrogel particle. This hydrogel display technique effectively maintained the genotype and phenotype linkage throughput the assay.

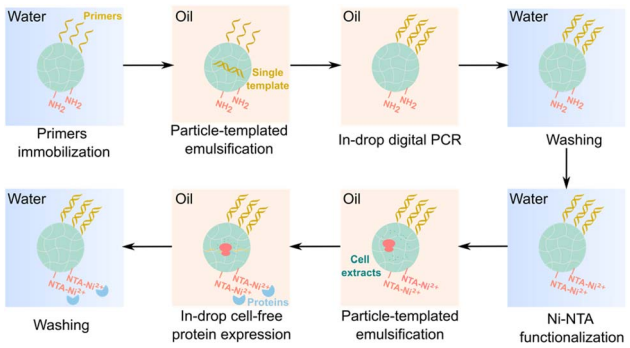

Fig. 1 Working principle of hydrogel particle-based protein display enabled by particle-templated emulsification.

3.2 Particle-templated emulsification

Polyacrylamide (PA) hydrogel particles were synthesized by copolymerizing acrylamide/bis-acrylamide and acrylate–PEG–NH_2 using a droplet microfluidic device. The resulting particles had an average diameter of 27.4 μm with a coefficient of variation of 2.6% (Fig. S1†). This high uniformity in particle size ensured consistent microreactor volumes, which are critical for reliable quantification in digital PCR and for uniform conditions in cell-free protein expression. Since these particles are pre-prepared and even commercially available, their production time does not impact the subsequent protein display efficiency.

The encapsulation of single hydrogel particles into droplets, which separated reactions into independent microreactors, plays an important role in maintaining the genotype and phenotype linkage and avoiding cross-contamination among different DNA variants. To achieve this, a simple and efficient particle-templated emulsification method was employed

Open Access Article. Published on 23 July 2025. Downloaded on 11/8/2025 4:52:06 AM.
This article is licensed under a Creative Commons Attribution-NonCommercial 3.0 Unported Licence.

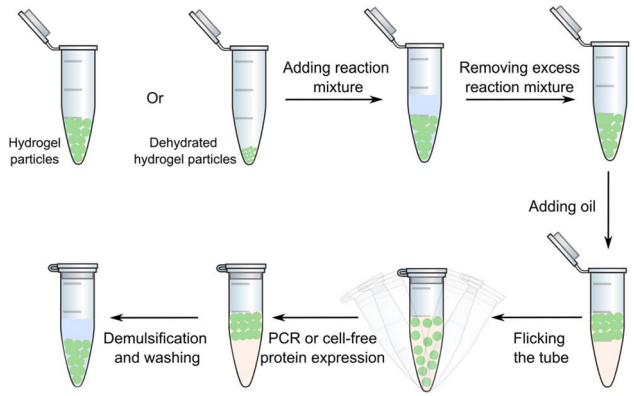

Fig. 2 Schematic of hydrogel particle-templated emulsification process.

(Fig. 2). Hydrogel particles were first incubated with reaction mixtures to allow absorption of reagents, after which excess aqueous phase was removed. Oil was then added, followed by vigorous agitation. During agitation, the particles were continuously partitioned into smaller droplets until further breakup was no longer possible, as it would require fracturing the gelled particles. As a result, the generated droplets were monodispersed, encapsulating single hydrogel particles that were similar in size to the templated particle. Subsequent reactions were then performed within these isolated hydrogel particles, ensuring efficient and contamination-free reactions. Fig. 3 and S2† shows that both macromolecules such as EGFP and small molecules such as FITC were successfully loaded into hydrogel particles and dispersed in the oil phase without cross-contamination with particle-templated emulsification.

Compared to conventional microfluidics-based emulsification, particle-templated emulsification is simpler and more user-friendly, as it does not require specialized equipment or expertise. The droplets generation speed is also faster, as particle-templated emulsification occurs simultaneously for all particles, keeping process time constant even when scaling up the aqueous phase volume. This scalability allows emulsification of both 20 μl and 2 ml volumes in about 30 seconds. In contrast, droplet microfluidics requires significantly more time as the volume increases; for instance, preparing 2 ml of 40 μm droplets can take approximately 11 hours.[38] In Fig. S3,† up to 10^9 hydrogel particles with diameters of 27 μm can be rapidly partitioned into emulsions in a 50 ml conical tube using particle-templated emulsification.[39] According to the Poisson distribution:

$$P(k) = \frac{\lambda^k e^{-\lambda}}{k!} \tag{1}$$

where $P(k)$ is the probability of encapsulating k molecules in a single droplet and λ is the average number of molecules per droplet. When λ is 0.1, approximately 9.05% of the droplets would contain a single DNA variant, enabling the screening of around 10^8 library variants. Thus, particle-templated emulsification provides a substantial time-saving advantage for large-volume emulsions.

Additionally, conventional droplet microfluidics often suffers from low single-particle encapsulation efficiency, whether for cells, beads, or pairing one cell with one bead, due to Poisson distribution.[49] For example, when the average number of particles encapsulated per droplet is 1, approximately 36.79% of the droplets remain empty, 36.79% contain a single particle, and 26.42% contain multiple particles (Fig. S4†). Reducing the average particle number per droplet to 0.1 significantly lowers the proportion of droplets containing multiple particles to just 0.47%. However, under this condition, 90.48% of the droplets are empty, and only 9.05% contain a single particle. Furthermore, the proportion of improperly loaded droplets increases dramatically when attempting to achieve precise one-to-one encapsulation. The probability of co-encapsulating k_1 particles and k_2 DNA molecules in a single droplet follows the product of two independent Poisson distributions:

$$P(k_1, k_2) = \frac{{\lambda_1}^{k_1} e^{-\lambda_1}}{k_1!} \times \frac{{\lambda_2}^{k_2} e^{-\lambda_2}}{k_2!} \tag{2}$$

where λ_1 is the average number of particles per droplet and λ_2 is the average number of DNA molecules per droplet. For instance, if $\lambda_1 = 1.0$ (to minimize empty droplets and ensure most droplets contain at least one particle) and $\lambda_2 = 0.1$ (to minimize multiple DNA occupancy), the probability of co-encapsulating exactly one particle and one DNA molecule is:

$$P(1, 1) = (\lambda_1 e^{-\lambda_1}) \times (\lambda_2 e^{-\lambda_2}) = (1 \times e^{-1}) \times (0.1 \times e^{-0.1}) \approx 3.33\% \tag{3}$$

Meanwhile, the probability of encapsulating at least one DNA molecule without any particle, which results in the loss of DNA variants during display due to lack of particle binding is:

$$P(0, k_2 \geq 1) = (e^{-\lambda_1}) \times (1 - e^{-\lambda_2}) = e^{-1} \times (1 - e^{-0.1}) \approx 3.50\% \tag{4}$$

Therefore, the inefficiency of conventional droplet microfluidics in achieving precise one-to-one pairing co-encapsulation leads to significant reagent waste and potential loss of DNA variants during protein display applications. In contrast, particle-templated emulsification offers nearly 100%

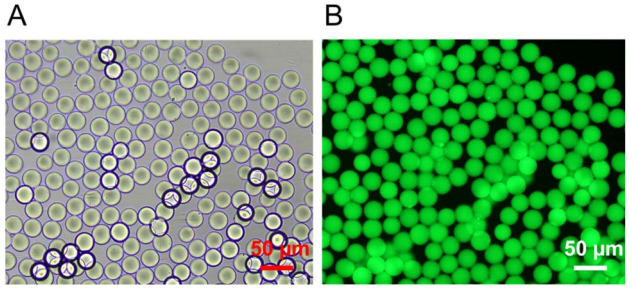

Fig. 3 EGFP was loaded into PA hydrogel particles, followed by dispersed into the oil phase using particle-templated emulsification. (A) Bright-field microscope image of the particles. (B) Fluorescence microscope image of the particles.

 © 2025 The Author(s). Published by the Royal Society of Chemistry

Open Access Article. Published on 23 July 2025. Downloaded on 11/8/2025 4:52:06 AM.
This article is licensed under a Creative Commons Attribution-NonCommercial 3.0 Unported Licence.

single-particle encapsulation efficiency. During the emulsification process, droplets containing multiple particles continue to break apart until only single-particle droplets remain. Under this system, with $\lambda_2 = 0.1$, the probability of co-encapsulating one particle and one DNA molecule increases to 9.05%, greatly improving pairing efficiency. Moreover, as long as all DNA solutions are fully absorbed by the hydrogel particles prior to emulsification, DNA loss during encapsulation can be effectively reduced.

3.3 In-drop digital PCR

To amplify the single DNA variant for protein synthesis, digital PCR was carried out in the hydrogel particles using particle-templated emulsification. PCR reagents, except for DNA templates, were first incubated with the hydrogel particles to allow absorption of reagents. After removing excess reagents, DNA templates were added, followed by particle-templated emulsification. Adding DNA templates only after removing excess PCR reagents minimized the risk of DNA diversity loss, ensuring high efficiency encapsulation of DNA templates within the hydrogel particles. In contrast, conventional droplet microfluidics often results in DNA diversity loss due to inefficient encapsulation of single DNA templates with single hydrogel particles in droplets. After forming emulsions, PCR was conducted in the hydrogel particles. In Fig. 4A, EvaGreen, which emits strong green fluorescence upon binding to double-stranded DNA, was used to visualize and confirm the presence of PCR products. The image demonstrates successful digital PCR within the hydrogel particles, as evidenced by some particles emitting green fluorescence, indicating amplification, while others remained dark, indicating the absence of DNA templates. These results confirm that through particle-templated emulsification, DNA templates can be effectively dispersed into individual hydrogel particles, and PCR can subsequently be performed to amplify the single DNA templates within each isolated hydrogel particle.

To further immobilize the genotype, specifically the PCR products onto the hydrogel, the hydrogel particles were functionalized to anchor primers before PCR (Fig. 4B). Since the PA hydrogel was copolymerized with acrylate–PEG–NH_2, the hydrogel was initially treated with glutaraldehyde and then reacted with 5′-NH_2-primer to immobilize the primers. The successful loading and immobilization of macromolecules in the hydrogel particles *via* glutaraldehyde conjugation was demonstrated by immobilizing HRP molecules, as shown in Fig. S5.† Furthermore, to address the high reactivity of unreacted aldehyde groups, which could interfere with subsequent digital PCR, the remaining aldehyde groups were neutralized with hexamethylenediamine, restoring stable amine groups that could withstand thermal cycling. After digital PCR, the hydrogel particles were demulsified, washed and stained with EvaGreen. In Fig. 5, hydrogel particles with immobilized primers exhibited digital PCR results, as some particles emitted green fluorescence while others did not (Fig. 5C and D). In contrast, hydrogel particles without primer functionalization failed to retain PCR products after demulsification, resulting in no fluorescent signal following washing (Fig. 5A and B). The results demonstrate that pre-immobilizing primers on the hydrogel particles is essential for retaining amplified DNA, thereby enabling genotype immobilization. Without proper primer anchoring, the PCR products would diffuse out of the particles, disrupting the genotype–phenotype linkage and compromising the integrity and accuracy of the display system.

3.4 In-drop cell-free protein expression

After digital PCR, DNA copies from single DNA templates were immobilized on the hydrogel particles and were ready for the following protein expression. To construct a stable genotype–phenotype linkage, it was essential to immobilize the expressed proteins on the same particle as their encoding genes. To enable protein capture and immobilization, hydrogel particles containing DNA copies and amine groups were further functionalized by reacting with glutaraldehyde, followed by treatment with AB-NTA and Ni^{2+} (Fig. 6A). The resulting Ni-NTA groups exhibit strong binding affinity for histidine-tagged proteins,

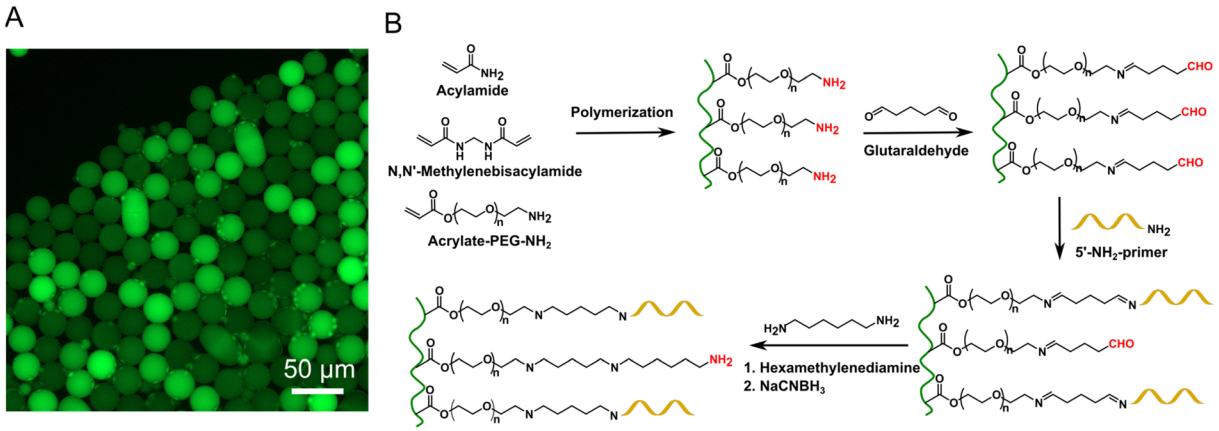

Fig. 4 (A) Digital PCR was conducted in hydrogel particle-templated emulsions using pUC57-Hoxal plasmid as a template. Hydrogel particles were stained with EvaGreen within the oil phase. (B) Hydrogel particle polymerization and functionalization to immobilize PCR products.

Open Access Article. Published on 23 July 2025. Downloaded on 11/8/2025 4:52:06 AM.
This article is licensed under a Creative Commons Attribution-NonCommercial 3.0 Unported Licence.

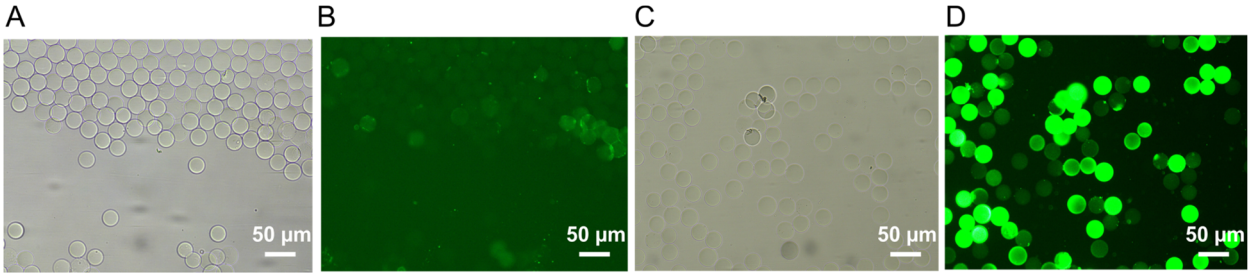

Fig. 5 In-drop digital PCR using pIVEX2.4C-mCherry plasmid as a template. (A) Bright-field microscope image and (B) fluorescence microscope image of unfunctionalized hydrogel particles after PCR and droplets demulsification. PCR products diffused into the aqueous phase, with no digital fluorescence signals observed in the hydrogel particles. (C) Bright-field microscope image and (D) fluorescence microscope image of functionalized hydrogel particles after PCR and droplets demulsification. PCR products were successfully immobilized on the hydrogel particles, which emitted strong green fluorescence due to EvaGreen staining.

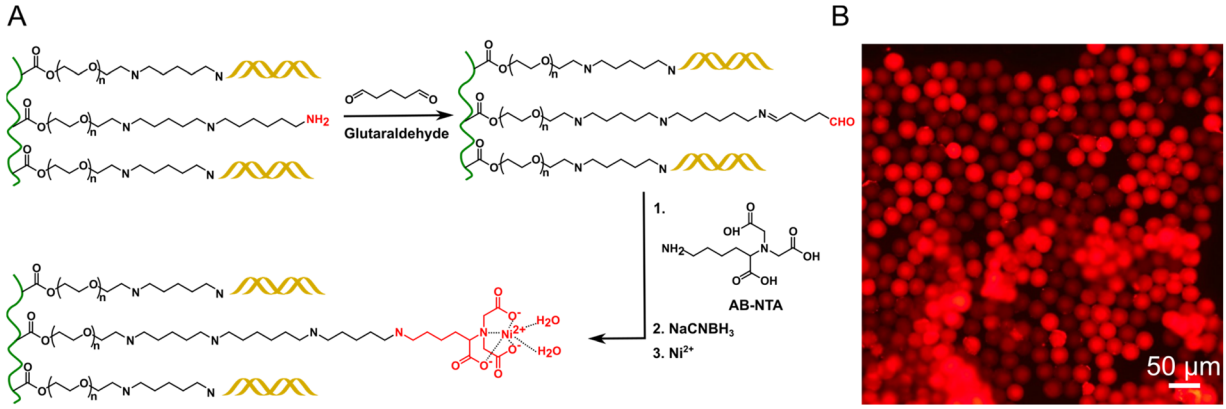

Fig. 6 (A) Hydrogel particle functionalization with Ni-NTA for protein immobilization. (B) In-drop cell-free protein expression. mCherry was expressed using immobilized digital PCR products as the template and was captured and immobilized on the hydrogel particle. Hydrogel particles were demulsified and washed before observing.

ensuring efficient capture and immobilization of the cell-free expressed histidine-tagged proteins. As shown in Fig. S6,† hydrogel particles functionalized with Ni-NTA successfully immobilized histidine-tagged EGFP, while particles without Ni-NTA failed to retain the protein, confirming that Ni-NTA groups on the hydrogel particles are essential for immobilizing histidine-tagged proteins.

After Ni-NTA functionalization, the hydrogel particles were freeze-dried and rehydrated with cell-free protein expression reagents. The rehydrated particles were then re-emulsified using particle-templated emulsification. Following in-drop cell-free protein expression, the droplets were demulsified and the particles were washed. As shown in Fig. 6B, some particles exhibited strong red fluorescence, which comes from the expressed mCherry protein, while others did not, indicating successful expression and immobilization of mCherry within the hydrogel particles. The observed bulk red fluorescence in Fig. 6B was due to the overlap of multiple hydrogel particles. Since cell-free protein expression occurred within individual hydrogel particles using immobilized digital PCR products as templates, a direct one-to-one correspondence was established between the DNA templates and the expressed proteins, creating a stable physical linkage between the genotype and phenotype. With both genotype and phenotype stably immobilized within the same hydrogel particles, protein display was effectively achieved, laying a foundation for downstream functional screening, such as enzyme evolution and affinity-based selection.

To verify the absence of cross-contamination between particles during the protein display process, plasmids encoding EGFP and mCherry were mixed at a 1 : 1 ratio and subjected to the hydrogel-based display workflow. As shown in Fig. S7A,† green fluorescence from EGFP and red fluorescence from mCherry were observed in different particles with no overlapping signals, indicating that cross-contamination did not occur during the display process. Furthermore, the comparable proportions of green- and red-fluorescent particles (Fig. S7B†) demonstrate that the display method does not introduce significant bias toward either genotype, thereby confirming the compartmentalization fidelity and reliability of the hydrogel display system.

The cell-free protein expression capability of the platform provides greater flexibility in the production of a wide range of proteins, especially those that are challenging to express *in vivo*, such as toxic proteins, membrane proteins and multimeric proteins.[50–52] To achieve efficient cell-free protein expression, the DNA templates were pre-amplified with PCR and the

 © 2025 The Author(s). Published by the Royal Society of Chemistry

Open Access Article. Published on 23 July 2025. Downloaded on 11/8/2025 4:52:06 AM. This article is licensed under a Creative Commons Attribution-NonCommercial 3.0 Unported Licence.

reactions were isolated within single hydrogel particles with sufficient reagents. Additionally, to reduce the steric hindrance of the hydrogel polymer chain during transcription, the primers were anchored onto the hydrogel through a long PEG chain, with molecular weight of 2000, enhancing the flexibility of PCR products chain, and thereby improving transcription efficiency.

Furthermore, the hydrogel particle, as the carrier for protein display, offers several distinct advantages. The solution-like nature of hydrogel creates a favorable environment for proteins by protecting and stabilizing their structures. Proteins are protected from degradation and denaturation, which is important in long-time studies.[53,54] For instance, when engineering enzymes with long-time activity, a suitable carrier to preserve their original activity is crucial. The three-dimensional structure of hydrogel, which facilitates high loading capacity of proteins, increases the protein product density, leading to less-biased results when selecting target proteins during display. The porous structure allows efficient mass transfer, making the hydrogel particle an ideal protein carrier for displaying. Substrates for protein analysis can easily interact with the displayed proteins, promoting efficient protein screening and selection. Finally, hydrogel particles can be easily manipulated and incorporated into various systems, such as fluorescence-activated cell sorting (FACS), droplet microfluidics, microwells, *et al.* for further manipulation or observation.[36,55] Leveraging the advantages of this hydrogel particle-based protein display platform, we aim to further investigate the evolution of proteins that are typically difficult to express *in vivo*, and engineer enzymes requiring specific selection stresses, such as long-term activity, organic solvent tolerance, and other stress conditions, or multi-parameter selection, which are often challenging in homogeneous *in vitro* display methods.

4. Conclusions

In this study, we have developed a hydrogel particle-based protein display method enabled by particle-templated emulsification. The emulsification process is rapid, user-friendly and highly efficient. Unlike conventional droplet microfluidics, particle-templated emulsification achieves higher single-particle encapsulation and improved one-to-one particle–DNA pairing efficiency. The emulsification time is independent of volume, as all emulsions are generated simultaneously through simple, instrument-free agitation. With particle-templated emulsification, a single DNA template was first emulsified with a single hydrogel particle, followed by digital PCR, resulting in hundreds of DNA template copies immobilized on the hydrogel particle. The particles were then re-emulsified to perform cell-free protein expression, where the expressed proteins were captured and immobilized on the same hydrogel particle as the DNA templates, forming a robust physical linkage between genotype and phenotype.

Compared to conventional *in vivo* protein display methods, such as phage display and cell surface display, cell-free protein expression overcomes challenges related to inefficient gene transformation and complexities of cell proliferation and viability. The use of isolated microreactors ensure that different DNA variants in the library produce a similar amount of protein by providing sufficient reagents and eliminating competition among different variants. This approach minimizes the expression biases commonly observed in homogeneous *in vitro* protein display systems, such as mRNA display and ribosome display. Additionally, using hydrogel particles as carriers for protein display enhances the stability and loading capacity of the displayed proteins, offers an accessible environment for protein interactions, and facilitates integration with various detection and sorting system, making hydrogel particles highly suitable for protein evolution, particularly in applications required compartmentalized screening. We anticipate that this hydrogel-based protein display method enabled by particle-templated emulsification will become a powerful tool in protein discovery and engineering.

Data availability

The authors confirm that the data supporting the findings of this study are available within the article and as its ESI.†

Author contributions

Han Wu: conceptualization, investigation, methodology, writing – original draft, supervision. Jiayao Fang: investigation, methodology. Jiao Chen: investigation, methodology. Yaoqi Wang: investigation, methodology. Bo Zheng: conceptualization, investigation, methodology, funding acquisition, writing – review & editing, supervision.

Conflicts of interest

There are no conflicts to declare.

Acknowledgements

We thank the financial support from Shenzhen Bay Laboratory (No. 21280031 and S211101001-5).

Notes and references

1 F. Chiti and C. M. Dobson, *Annu. Rev. Biochem.*, 2017, **86**, 27–68.
2 L. T. Bergendahl, L. Gerasimavicius, J. Miles, L. Macdonald, J. N. Wells, J. P. I. Welburn and J. A. Marsh, *Protein Sci.*, 2019, **28**, 1400–1411.
3 S. B. Ebrahimi and D. Samanta, *Nat. Commun.*, 2023, **14**, 1–11.
4 B. Leader, Q. J. Baca and D. E. Golan, *Nat. Rev. Drug Discovery*, 2008, **7**, 21–39.
5 A. Madhavan, K. B. Arun, P. Binod, R. Sirohi, A. Tarafdar, R. Reshmy, M. Kumar Awasthi and R. Sindhu, *Bioresour. Technol.*, 2021, **325**, 124617.
6 J. L. Porter, R. A. Rusli and D. L. Ollis, *ChemBioChem*, 2016, **17**, 197–203.
7 M. Eisenstein, *Nat. Biotechnol.*, 2023, **41**, 303–305.

Open Access Article. Published on 23 July 2025. Downloaded on 11/8/2025 4:52:06 AM.
This article is licensed under a Creative Commons Attribution-NonCommercial 3.0 Unported Licence.

8 A. Miserez, J. Yu and P. Mohammadi, *Chem. Rev.*, 2023, **123**, 2049–2111.
9 J. L. Watson, D. Juergens, N. R. Bennett, B. L. Trippe, J. Yim, H. E. Eisenach, W. Ahern, A. J. Borst, R. J. Ragotte, L. F. Milles, B. I. M. Wicky, N. Hanikel, S. J. Pellock, A. Courbet, W. Sheffler, J. Wang, P. Venkatesh, I. Sappington, S. V. Torres, A. Lauko, V. De Bortoli, E. Mathieu, S. Ovchinnikov, R. Barzilay, T. S. Jaakkola, F. DiMaio, M. Baek and D. Baker, *Nature*, 2023, **620**, 1089–1100.
10 J. Durairaj, A. M. Waterhouse, T. Mets, T. Brodiazhenko, M. Abdullah, G. Studer, G. Tauriello, M. Akdel, A. Andreeva, A. Bateman, T. Tenson, V. Hauryliuk, T. Schwede and J. Pereira, *Nature*, 2023, **622**, 646–653.
11 B. Fram, Y. Su, I. Truebridge, A. J. Riesselman, J. B. Ingraham, A. Passera, E. Napier, N. N. Thadani, S. Lim, K. Roberts, G. Kaur, M. A. Stiffler, D. S. Marks, C. D. Bahl, A. R. Khan, C. Sander and N. P. Gauthier, *Nat. Commun.*, 2024, **15**, 5141.
12 T. Kortemme, *Cell*, 2024, **187**, 526–544.
13 H. W. Hellinga, *Proc. Natl. Acad. Sci. U. S. A.*, 1997, **94**, 10015–10017.
14 M. S. Packer and D. R. Liu, *Nat. Rev. Genet.*, 2015, **16**, 379–394.
15 M. Li, *Nat. Biotechnol.*, 2000, **18**, 1251–1256.
16 M. S. Newton, Y. Cabezas-Perusse, C. L. Tong and B. Seelig, *ACS Synth. Biol.*, 2020, **9**, 181–190.
17 M. Park, *Sensors*, 2020, **20**, 2775.
18 G. P. Smith and V. A. Petrenko, *Chem. Rev.*, 1997, **97**, 391–410.
19 S. Y. Lee, J. H. Choi and Z. Xu, *Trends Biotechnol.*, 2003, **21**, 45–52.
20 C. N. Grun, R. Jain, M. Schniederberend, C. B. Shoemaker, B. Nelson and B. I. Kazmierczak, *Nat. Commun.*, 2024, **15**, 7502.
21 E. van Bloois, R. T. Winter, H. Kolmar and M. W. Fraaije, *Trends Biotechnol.*, 2011, **29**, 79–86.
22 W. Jaroszewicz, J. Morcinek-Orłowska, K. Pierzynowska, L. Gaffke and G. Węgrzyn, *FEMS Microbiol. Rev.*, 2022, **46**, 1–25.
23 D. Lipovsek and A. Plückthun, *J. Immunol. Methods*, 2004, **290**, 51–67.
24 Y. Zeng, M. Woolley, K. Chockalingam, B. Thomas, S. Arora, M. Hook and Z. Chen, *Nucleic Acids Res.*, 2023, **51**, E89.
25 C. Zahnd, P. Amstutz and A. Plückthun, *Nat. Methods*, 2007, **4**, 269–279.
26 M. J. Hammerling, B. R. Fritz, D. J. Yoesep, D. S. Kim, E. D. Carlson and M. C. Jewett, *Nat. Commun.*, 2020, **11**, 1–10.
27 J. Hanes and A. Plückthun, *Proc. Natl. Acad. Sci. U. S. A.*, 1997, **94**, 4937–4942.
28 J. W. Keum, J. H. Ahn, C. Y. Choi, K. H. Lee, Y. C. Kwon and D. M. Kim, *Biochem. Biophys. Res. Commun.*, 2006, **350**, 562–567.
29 J. H. Ahn, J. W. Keum and D. M. Kim, *J. Proteome Res.*, 2008, **7**, 2107–2113.
30 K. H. Lee, K. Y. Lee, J. Y. Byun, B. G. Kim and D. M. Kim, *Lab Chip*, 2012, **12**, 1605–1610.
31 J. Y. Byun, K. H. Lee, K. Y. Lee, M. G. Kim and D. M. Kim, *Lab Chip*, 2013, **13**, 886–891.
32 D. A. Weitz, R. Assaf, C. Shaorong and H. John, Hydrogel display, PCT Patent, WO2018/067789A1, 2018.
33 T. Tang, H. Zhao, S. Shen, L. Yang and C. T. Lim, *Microsyst. Nanoeng.*, 2024, **10**, 3.
34 D. Liu, M. Sun, J. Zhang, R. Hu, W. Fu, T. Xuanyuan and W. Liu, *Analyst*, 2022, **147**, 2294–2316.
35 E. Brouzes, M. Medkova, N. Savenelli, D. Marran, M. Twardowski, J. B. Hutchison, J. M. Rothberg, D. R. Link, N. Perrimon and M. L. Samuels, *Proc. Natl. Acad. Sci. U. S. A.*, 2009, **106**, 14195–14200.
36 D. Koveal, P. C. Rosen, D. J. Meyer, C. M. Díaz-García, Y. Wang, L. H. Cai, P. J. Chou, D. A. Weitz and G. Yellen, *Nat. Commun.*, 2022, **13**, 2919.
37 D. W. Weisgerber, M. N. Hatori and A. R. Abate, *J. Visualized Exp.*, 2021, **2021**, 1–12.
38 M. N. Hatori, S. C. Kim and A. R. Abate, *Anal. Chem.*, 2018, **90**, 9813–9820.
39 I. C. Clark, K. M. Fontanez, R. H. Meltzer, Y. Xue, C. Hayford, A. May-Zhang, C. D'Amato, A. Osman, J. Q. Zhang, P. Hettige, J. S. A. Ishibashi, C. L. Delley, D. W. Weisgerber, J. M. Replogle, M. Jost, K. T. Phong, V. E. Kennedy, C. A. C. Peretz, E. A. Kim, S. Song, W. Karlon, J. S. Weissman, C. C. Smith, Z. J. Gartner and A. R. Abate, *Nat. Biotechnol.*, 2023, **41**, 1557–1566.
40 S. L. Anna, N. Bontoux and H. A. Stone, *Appl. Phys. Lett.*, 2003, **82**, 364–366.
41 S. Y. Teh, R. Lin, L. H. Hung and A. P. Lee, *Lab Chip*, 2008, **8**, 198–220.
42 X. Zhou, H. Wu, M. Cui, S. N. Lai and B. Zheng, *Chem. Sci.*, 2018, **9**, 4275–4279.
43 Y. Xia and G. M. Whitesides, *Angew. Chem.*, 1998, **37**, 550–575.
44 G. M. Whitesides, E. Ostuni, S. Takayama, X. Jiang and D. E. Ingber, *Annu. Rev. Biomed. Eng.*, 2001, **3**, 335–373.
45 M. W. Nirenberg and J. H. Matthaei, *Proc. Natl. Acad. Sci. U. S. A.*, 1961, **47**, 1588–1602.
46 Y. Shimizu, A. Inoue, Y. Tomari, T. Suzuki, T. Yokogawa, K. Nishikawa and T. Ueda, *Nat. Biotechnol.*, 2001, **19**, 751–755.
47 E. D. Carlson, R. Gan, C. E. Hodgman and M. C. Jewett, *Biotechnol. Adv.*, 2012, **30**, 1185–1194.
48 T. Okano, T. Matsuura, Y. Kazuta, H. Suzuki and T. Yomo, *Lab Chip*, 2012, **12**, 2704–2711.
49 L. Mazutis, J. Gilbert, W. L. Ung, D. A. Weitz, A. D. Griffiths and J. A. Heyman, *Nat. Protoc.*, 2013, **8**, 870–891.
50 F. Katzen, T. C. Peterson and W. Kudlicki, *Trends Biotechnol.*, 2009, **27**, 455–460.
51 X. Jin and S. H. Hong, *Biochem. Eng. J.*, 2018, **138**, 156–164.
52 D. Garenne, M. C. Haines, E. F. Romantseva, P. Freemont, E. A. Strychalski and V. Noireaux, *Nat. Rev. Methods Primers*, 2021, **1**, 49.
53 M. Nöth, E. Gau, F. Jung, M. D. Davari, I. El-Awaad, A. Pich and U. Schwaneberg, *Green Chem.*, 2020, **22**, 8183–8209.
54 J. Meyer, L. E. Meyer and S. Kara, *Eng. Life Sci.*, 2022, **22**, 165–177.
55 M. Fischlechner, Y. Schaerli, M. F. Mohamed, S. Patil, C. Abell and F. Hollfelder, *Nat. Chem.*, 2014, **6**, 791–796.

 © 2025 The Author(s). Published by the Royal Society of Chemistry